14th Asia-Pacific Conference on Combustion
Kaohsiung Exhibition Center, Kaohsiung, Taiwan
14th-18th May 2023

Understanding the Thermal Behaviour of Electrically Controlled Solid Propellant with Different Metal Additives

Rajendra Rajak[1], Daehong Lim[1], Kanagaraj Gnanaprakash[2], Jack J. Yoh[1*]

[1]Department of Aerospace Engineering, Seoul National University, Seoul, 08826, South Korea

[2]Department of Mechanical and Aerospace Engineering, Indian Institute of Technology Hyderabad
Kandi, Telangana, 502284, India

Abstract

Electrically controlled solid propellant (ECSP) has been investigated from past many decades but not enough effort has been given to understand the physio-chemical mechanism of the ECSP burning and thermal behaviour on addition of different metal additives. This paper enunciates the effect of different metal additives viz. Aluminium(Al), Magnesium(Mg) and Titanium(Ti) mixed in the ECSP baseline composition, with lithium perchlorate (LP) as the oxidizer and polyvinyl alcohol (PVA) as binder. Addition of different metals affects the thermal stability of the ECSP combustion. ECSP with three different metal additives was synthesized and the burning experiments of each sample under atmospheric condition were done to understand the flame behaviour. Thermal analysis using differential scanning calorimetry (DSC), thermogravimetric analysis (TGA) reveals the thermal stability and associated mass loss of the considered ECSP's. It is noticed that the decomposition of the Mg based ECSP occurs at higher temperature range as compared to Ti and Al based ECSP. Surface morphology of the aforementioned composition were observed and their elemental mapping using EDS was conducted. It is noticed that the lithium perchlorate- polyvinyl alcohol based baseline composition is not the universal composition to accommodate any metal additives, furthermore the burning ceases when the magnesium is added to the baseline.

1 Introduction

Electrically controlled solid propellants are the special class of propellants which ignites only when sufficient amount of electric power is applied externally and the combustion completely ceases when there is absence of electric power. This pyroelectric behaviour of ECSP makes them to use it as a multiple start and stop bits in the space application for controlling the attitude of the satellite by utilizing these ECSP in the micro thrusters, pulsed plasma thrusters, gas generator systems and long range rocket motors. Owing to their higher stability, controllable throttle, establishing multiple impulse bits and adjustable burning rate by altering the electrical power supply, ECSP can also be utilized in future to design a highly stable rocket motors with wide range of operating frequencies.

Sawka et al. [1] synthesized hydroxyl ammonium nitrate (HAN) based composition and had demonstrated ECSP utility in micro to macro propulsion technology by performing the experiments up to 6.8 MPa in a closed bomb setup. They found out that after 1.36 MPa the ECSP burning is self-sustaining which is a drawback. Throttling of the propellant burning rate is accomplished by changing the electrical power input.

Bao et al. [2] studied the effect of graphite as an additive to the HAN based ECSP and found that the introduction of the carbon increases the thermal conductivity but at the expense of adiabatic flame temperature reduction which thereby reduces the specific impulse (Isp) of the propellant. They have also conducted the research on ECSP by varying the initial temperature (-15°C, 5°C, 25°C and 45°C) of the propellant [2]. Raising the initial temperature of the ECSP enhances the decomposition and vaporization at the burning area thereby increasing the regression rate. Gnanaprakash et al. [3] has adopted the similar baseline composition (LP/PVA based) as He et al. [4] with difference in the metal additive as Tungsten (W) and to improve the mechanical properties of the ECSP, they included glycerol and boric acid. Addition of W decreased the decomposition temperature by 60°C compared to non- metallized ECSP. It is also noticed that the thermal stability of the ECSP reduced due to the inclusion of the W particles. He et al. [4] performed the experiments on the lithium perchlorate (LP) and polyvinyl alcohol (PVA) based ECSP with aluminium as a metal additive, in the pressure range of 0.1 – 5 MPa, with aluminium powder below 20% in the composition. LP based ECSP has shown higher thermal stability and high electrical control relative to HAN based composition which is hygroscopic in nature. $LiClO_4$/PVA/H_2O had weight ratio of 1/0.43/0.36, 1.0/0.67/0.42 and 1.0/1.0/0.5, with aluminium powder less than 20 % in their composition.

Glascock et al. [4, 5] formulated the HAN and PVA based ECSP and studied the ablation of ECSP due to the arc discharge and found out that these ECSP has higher specific ablation per pulse and since HAN is hygroscopic in nature, the surface layer in the hygroscopic ECSP is rapidly ablated which decreases the average specific impulse.

Gobin et al. [7] characterized ECSP using the polymer electrolytes with different percentage of polyethylene oxide (PEO), LP and ammonium perchlorate (AP). It is observed that the magnitude of the applied voltage is the dictating factor for the burning rate of the ECSP. It was further noticed that the decomposition always initiated at the negatively charged cathode. The formation of the liquid decomposition layer which when spread to the anode accelerates the decomposition of the perchlorate ions. Baird et al. [8] has reported about the effect of variation in the electrode area ratio, that dictates where the preferential burning of the ECSP (HAN + PVA based) would take place. Combustion

*Corresponding author, Fax: +82-2-882-1507
E-mail address: jjyoh@snu.ac.kr (J.J. Yoh)

always takes place at the smaller electrode irrespective of the polarity of the electrodes.

It is evident from the literature that not enough work has been reported in exploring the effect of various metal content in the ECSP composition compared to the conventional propellant. In this paper the effect of various metal additives on combustion when blended with the baseline composition of the ECSP and their thermal analysis are investigated. No such studies have been reported in the past and this study is an attempt to comprehend the metal effect on ECSP.

2 Experimental Section

2.1 Propellant preparation

The main ingredients of ECSP samples are lithium perchlorate (Alfa Aesar Ltd.) with purity of 99.0% as an oxidizer, polyvinyl alcohol (Sigma-Aldrich Ltd.) with molecular weight of 146,000–186,000 and degree of hydrolysis > 99.0% as binder/fuel, and boric acid (H3BO3) as cross-linking agent. Magnesium (US Research Nanomaterials Inc.) with a particle size of 10 µm, Titanium (US Research Nanomaterials Inc.) with a particle size of 800 nm and Aluminium (US Research Nanomaterials) with a particle size of 10 µm are used as a metal fuel additive. Different compositions of ECSP were synthesized to understand the effect of different metal additive. During the propellant preparation the weight ratio of the LP and water was maintained to be 1:1.85 which is marginally greater than the solubility limit. Three different compositions were made with Mg as 5% in first composition, 1% Ti in second composition and 1% Al in third composition, compositions used in this study are shown in Table 1. The propellant ingredients were mixed using a planetary centrifugal mixer (Thinky ARE-310, Japan) for total of 45 minutes for homogenizing the ingredients after LP and PVA are dissolved in the water.

Table 1: ECSP composition.

Ingredients	M0 (mass in g) Baseline	M1 (aluminium based, 1%)	M1 (Titanium based, 1%)	M5 (Magnesium based, 5%)
Distilled water	5.388	5.3228	5.3228	5.063
LP	2.912	2.8772	2.8772	2.737
PVA	1.0	1.0	1.0	1.0
Metal	0.0	0.1	0.1	0.5
Glycerol	0.5	0.5	0.5	0.5
Boric acid	0.2	0.2	0.2	0.2

2.2 Characterization methods

Thermal analysis of the ECSP samples were performed using differential scanning calorimetry (DSC 3+, Mettler Toledo) and thermogravimetry (TGA 2, Mettler Toledo) to characterize the ECSP samples at different heating rates. For DSC experiments, ECSP sample of weight ~ 1mg was kept inside the 40 µl Al crucible and sealed with the perforated covering and keeping the standard nitrogen flow of 40 ml/min. Observation temperature for the DSC analysis was in the range of 30 °C – 600 °C. Two different heating rates of 10 °C /min and 20 °C /min was selected to investigate the decomposition of the ECSP samples. TGA experiments were conducted with the 40 µl Al crucible unsealed and ~ 1mg of the sample was kept inside it for its analysis. Temperature range between 35 °C – 500 °C was considered with heating rates of 10 °C /min and 20 °C /min for TGA experiments. All experimental conditions and procedures followed the International Confederation for Thermal Analysis and Calorimetry Kinetics Committee's recommendations.

Scanning Electron Microscopy- Energy Dispersive Spectroscopy (SEM-EDS) analysis has also been performed to observe the surface morphology of the ECSP samples and EDS provides the elemental mapping of these ECSP samples. To accomplish this task a field emission scanning electron microscope (FE-SEM, make ZEISS GeminiSEM 560, ZEISS, Germany) with a resolution of 0.5 nm at 15 kV was utilized. GeminiSEM 560 is equipped with a Gemini column designed with Schottky type field emission and in column beam deceleration design, enabling high- resolution image and surface morphology observation at low acceleration voltage without stage bias by implementing a field-free objective lens. In addition, by implementing 8.5 mm analytical working distance, EDS signal acquisition is excellent and good mapping results can be derived.

2.3 ECSP flame visualization

To visualize the flame, the combustion of these synthesized ECSP were done under open atmospheric conditions and the video was recorded using DSLR camera with 24 frames per second (fps). The setup to burn the ECSP under open atmospheric condition is shown in Fig.1. Setup consist of bottom electrode made of Molybdenum and the top electrode is made of Nichrome wire. The bottom electrode is supported with teflon plate to provide proper insulation. The ECSP sample is ignited using the high voltage DC supply, varying the voltage alters the burning rate of the ECSP sample.

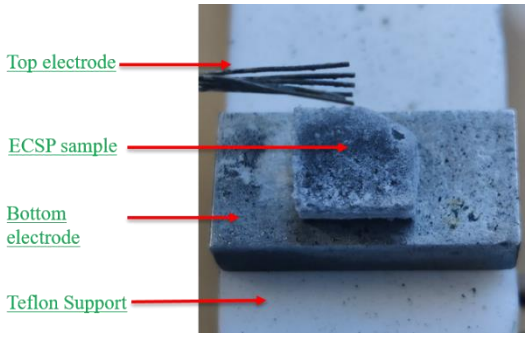

Figure 1: Setup to visualize the ECSP flame under atmospheric conditions.

3 Results and Discussion

3.1 Surface morphology

Surface morphology of three metallized ECSP samples were performed using the SEM and their elemental mapping was conducted using EDS technique. The SEM-EDS of the magnesium based ECSP is shown in Fig.2. Based on the physical appearance of the slurry formed after the mixing of the propellant ingredients was without any air bubbles, blow holes or voids which ensure that the mixing was proper. Once the

curing is done, the samples protrusion and irregularity were the results of the evaporation of the water content in the ECSP sample. SEM images shows the homogeneity obtained while synthesizing the sample and the EDS mapping of the residue from the thermal analysis experiments shows the elemental mapping corresponding to the ECSP sample.

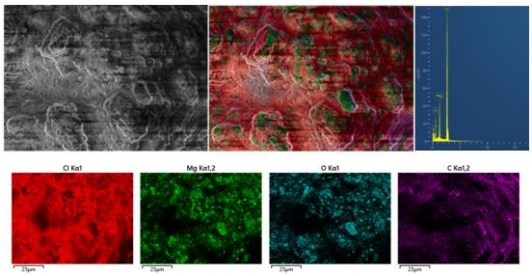

Figure 2: SEM image and EDS mapping of residues from thermal experiments for Mg based composition.

Different elements in the EDS mapping include C, O, Cl and Mg. Lithium cannot be identified from the EDS analysis, so the presence of the Cl in the EDS mapping indicate the existence of LiCl in the composition.

3.2 Thermal analysis

DSC and TGA of the three different metallized based ECSP has been conducted to obtain the heat of reaction and understand the thermal stability of these samples. The DSC, TGA and dTG curves for Mg, Al and Ti based ECSP samples at heating rates of 10 °C/min and 20 °C/min are shown in Fig.3, Fig.4, Fig.5, Fig.6, Fig.7 and Fig.8. DSC experiments were conducted in the temperature range of 30 °C – 600 °C with two different heating rates of 10 °C/min and 20 °C/min under the nitrogen ambience. DSC curve of all the ECSP samples shows an endothermic peak at 98 °C. The endothermic peaks at heating rates of 20 °C/min are more pronounces as compared to the DCS curves of all the ECSP samples at the heating rate of 10 °C/min. In both the heating rates of 10 °C/min and 20 °C/min, it is seen that the decomposition temperature of the aluminium and titanium based ECSP samples fall in the temperature range of 280 °C to 380 °C. At heating rate of 10 °C/min, it is noticed that the second exothermic peak for the titanium based ECSP is observed above 400 °C. Similar observation is not noticed for the titanium based ECSP at the heating rate of 20 °C/min. The relative mass loss for all the ECSP compositions, at different heating rates during the first endothermic peak at the DSC curve, is up to 10 %, and this mass loss is due to the evaporation of the water in all the ECSP samples considered in this study.

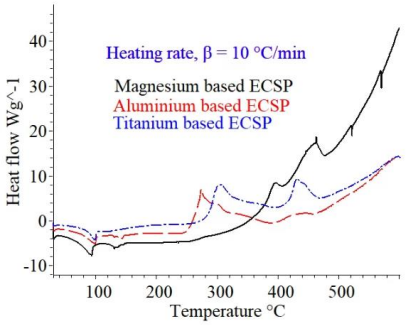

Figure 3: DSC curve for Mg, Al and Ti based ECSP at heating rate of 10 °C/min.

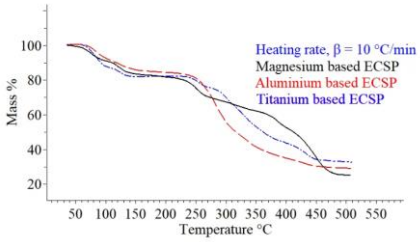

Figure 4: TGA curve for Mg, Al and Ti based ECSP at heating rate of 10 °C/min.

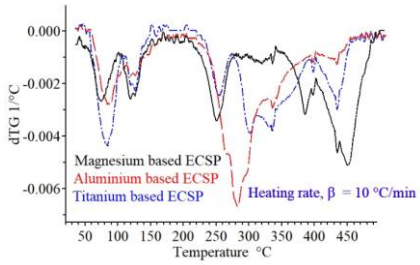

Figure 5: dTG curve for Mg, Al and Ti based ECSP at heating rate of 10 °C/min.

The decomposition of the aluminium and titanium based ECSP initiates at around 280 °C, exothermic peaks can be seen between the temperature range of 280 °C to 380 °C. A significant amount of mass loss happens to the aluminium based ECSP as compare to the titanium based ECSP. For aluminium based ECSP the mass loss after the decomposition is around 80 % and for titanium based ECSP the mass loss after the decomposition is around 50 %. This means that the thermal stability of the aluminium based ECSP is less relative to the titanium based ECSP. Decomposition of the magnesium based ECSP starts at the temperature around 380 °C at the heating rate of 10 °C/min and it starts at around 400 °C for the heating rate of 20 °C/min. It is noticed that the thermal stability of the magnesium based ECSP is higher than any other composition considered in this study. Table 2 lists the heat of reaction and the mass loss during the thermal analysis of the various ECSP samples considered in this study.

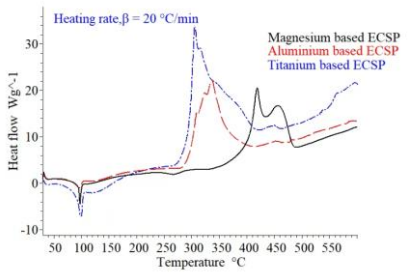

Figure 6: DSC curve for Mg, Al and Ti based ECSP at heating rate of 20 °C/min.

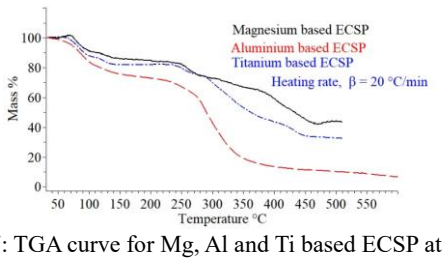

Figure 7: TGA curve for Mg, Al and Ti based ECSP at heating rate of 20 °C/min.

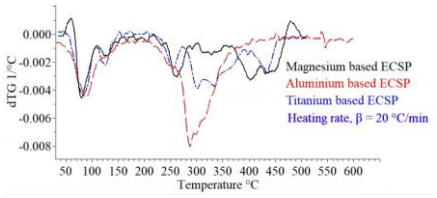

Figure 8: dTG curve for Mg, Al and Ti based ECSP at heating rate of 20 °C/min.

Table 2: Heat of reaction and mass loss for different ECSP samples.

Samples	Average heat of reaction (J/g)	Average mass loss (%)	Heating rate (℃/min)	Decomposition temperature (℃)
Mg (5%)_ECSP	1862.9	55 & 65	10	389 & 462
Al (1%)_ ECSP	2552.17	22	10	275
Ti (1%)_ ECSP, First peak	1860.89	22	10	303
Ti (1%)_ ECSP, second peak	892.78	61	10	431
Al (1%)_ ECSP	2413.42	80	20	336.29
Mg (5%)_ECSP	2082	57 & 65	20	418.76 & 459.58
Ti (1%)_ ECSP	4209	30	20	305

Table 2 compares the heat of reaction, % mass loss and decomposition temperature for the two different heating rates are considered in this study. The decomposition temperature for the magnesium based ECSP is always above 400 ℃. When compared to previous ECSP samples with different metal additions, it has been shown that the thermal stability of the magnesium-based ECSP is significantly more prominent. The decomposition of the magnesium-based ECSP sample takes place between 400 °C and 500 °C, whereas the decomposition of the titanium and aluminum-based ECSP samples takes place between 300 °C and 400 °C.

3.3 Combustion flame visualization

The burning of the ECSP samples at low voltages forms a liquid layers which rapidly spreads over the combustion zone thereby enhancing the electrical conductivity and thus further assisting the better uniform combustion. The formation of the condensed phase liquid is only seen at the low voltage conditions and not at the high voltage conditions. The propellant was kept in the open atmosphere on top of the molybdenum electrode connected to the negative wire of the DC power source. The positive wire of the DC power source was connected to the nichrome wire which acted as the second electrode. The polarity of the nichrome wire electrode was changed from positive to negative in the subsequent experiments to check where the preferential burning occurs. It is noticed that the burning happens at the electrode where the less area is in contact with the propellant and this phenomenon has been reported by Baird et al. [8].

Figure 9: Time sequential burning of Ti based ECSP sample.

Tests were conducted for the two different voltage values i.e., 300 V and 200 V. Figure 9 shows the sequential burning of the titanium based ECSP under the open atmospheric conditions. The ECSP flame looks very sooty and thus the flame color is bright yellow.

4 Conclusions

In this work, three distinct metal additions to the ECSP samples are characterized. The characterization is performed through DSC and TGA analysis. The thermal stability of the magnesium-based ECSP samples is found to be greater than that of the aluminum- or titanium-based ECSP samples. It is observed that the thermal decomposition of the aluminium and titanium based ECSP occurs in the similar temperature range of 280 ℃ to 380 ℃. But for the magnesium based ECSP the decomposition always happens after 400 ℃. This implies that the magnesium based ECSP composition have relatively higher thermal stability as compare to aluminium or titanium based ECSP. Additionally, it is seen that the formation of the liquid layer during the localized combustion of the ECSP samples under atmospheric conditions improves conduction. The electrical power supplied for combustion influences the burning rate of the ECSP samples; the higher the electric power, the faster the burning rate.

5 Acknowledgment

This work is financially supported by the National Research Foundation of Korea (NRF-0498-20210020), contracted through IAAT and IOER at Seoul National University.

References

[1] W. Sawka, M. McPherson, Electrical Solid Propellants: A Safe, Micro to Macro Propulsion Technology. 49th AIAA/ASME/SAE/ASEE Jt. Propuls. Conf., 2013, 1 PartF, p. 1–21.

[2] L. Bao, H. Wang, Z. Wang, H. Xie, S. Xiang, X. Zhang, W.Zhang, Y. Huang, R. Shen, Y. Ye, Combust. Flame, 236 (2022), 111804.

[3] K. Gnanaprakash, M.Yang, J.J. Yoh, Combust. Flame, 238 (2022), 111752.

[4] Z.He, Z. Xia, J. Hu, Y. Li, J. Propuls. Power, 35 (3) (2019), 512–519.

[5] M.S. Glascock, J.L. Rovey, K.A. Polzin, Aerospace, 7 (6) (2020), 1–19.

[6] M.S. Glascock, J.L. Rovey, K.A. Polzin, J. Propuls. Power, 35 (5) (2019), 984–993.

[7] B. Gobin, N. Harvey, G. Young, Combust. Flame, 2022, 244, 112291.

[8] J.K. Baird. J.R. Lang, A.T. Hiatt, R.A. Fredrick, J. Propuls. Power, 33 (6) (2017), 1589-1590.